

Theory of the electro-optical properties of graphene nanoribbons

Kondayya Gundra* and Alok Shukla

Department of Physics, Indian Institute of Technology, Bombay, Mumbai 400076, India

(Received 12 November 2010; revised manuscript received 31 December 2010; published 10 February 2011)

We present calculations of the optical absorption and electroabsorption spectra of graphene nanoribbons (GNRs) using a π -electron approach, incorporating long-range Coulomb interactions within the Pariser-Parr-Pople-model Hamiltonian. The approach is carefully benchmarked by computing quantities, such as the band structure, electric-field-driven half-metallicity, and linear optical absorption spectra of GNRs of various types, and the results are in good agreement with those obtained using *ab initio* calculations. Our predictions on the linear absorption spectra for the transversely polarized photons provide a means to characterize GNRs by optical probes. We also compute the electroabsorption spectra of the zigzag GNRs and argue that it can be used to determine whether or not they have a magnetic ground state, thereby allowing the edge magnetism to be probed through nonmagnetic experiments.

DOI: [10.1103/PhysRevB.83.075413](https://doi.org/10.1103/PhysRevB.83.075413)

PACS number(s): 78.20.Bh, 73.22.Pr, 78.40.Ri, 78.67.Wj

I. INTRODUCTION

The discovery of graphene¹ has stimulated intense research in the field from the point of view of both fundamental physics and promising applications.²⁻⁴ Of particular interest are recently synthesized⁵ quasi-one-dimensional (1D) nanostructures of graphene called graphene nanoribbons (GNRs), which have technologically promising electronic and optical properties because of the confinement of electrons owing to the reduced dimensions. As a result, numerous theoretical studies of electronic, transport, and optical properties of GNRs of various type have been performed over the years.⁶⁻¹⁶ The structural anisotropy of GNRs must exhibit itself in an anisotropic optical response with respect to the photons polarized along the length of the ribbons (x polarized, or longitudinally polarized) as against those polarized perpendicular to it (y polarized, or transversely polarized), with GNRs being in the xy plane. Despite its obvious importance, anisotropy in the optical response of GNRs has not been studied in any of the reported optical absorption calculations, which concentrate only on the longitudinal component of the spectra.¹²⁻¹⁶ In this paper we study this anisotropy in detail and make predictions that can be tested in optical experiments on oriented samples of GNRs and can serve as a means for their optical characterization.

Electroabsorption (EA) spectroscopy, which consists of measuring optical absorption in the presence of a static external electric (E) field, has been used extensively to probe the electronic structure and optical properties of conjugated polymers and other materials.¹⁷ GNRs, being π -conjugated systems, will also be amenable to similar EA probes, and, therefore, we have calculated the EA spectrum of zigzag GNRs (ZGNRs) in this work. ZGNRs have been predicted to possess a magnetic ground state, with oppositely oriented spins localized on the opposite zigzag edges of the ribbons.^{6,8} Our calculated EA spectra of ZGNRs depend strongly on whether or not they exhibit edge magnetism, thereby allowing their detection by optical means.

Most of the theoretical approaches used to study the electronic structure of GNRs are broadly based upon (a) the

tight-binding method,^{6,7,9} (b) the Dirac equation approach, derived using the linearity of the band structure in the region of interest,¹⁸ (c) the *ab initio* density-functional theory (DFT) and Green's function based GW approaches,^{10,11,13,15} and (d) the Hubbard-model-based approaches.¹⁹⁻²² However, it is obvious from the chemical structure of graphene and GNRs that the electrons close to the chemical potential are itinerant π electrons which determine their low-energy excitations. In π -electron systems, such as various aromatic molecules and conjugated polymers, it is well known that role of electron-electron ($e-e$) interactions cannot be ignored when describing their electronic properties.²³ Therefore, it is inconceivable that the long-range $e-e$ interactions will be insignificant in graphene and related structures. The effective π -electron approaches, such as the Pariser-Parr-Pople (PPP) model Hamiltonian,²⁴ which incorporate the long-range $e-e$ interaction, have been used with considerable success in describing the physics of π -conjugated molecules and polymers.²³ Computationally speaking, the PPP model has the advantage of including the long-range Coulomb interactions of π electrons within a minimal basis, thereby allowing calculations on such systems with limited computer resources, as compared to the *ab initio* approaches. Indeed, in our earlier papers, we have used the PPP model to extensively study the electronic structure and optical properties of *finite* π -electron systems, such as conjugated molecules and oligomers at various levels of theory.²⁵ Therefore, in this work, we have decided to extend our PPP-model-based approach to study the physics of GNRs in the bulk limit. Because, to the best of our knowledge, this is the first application of the PPP model to GNR physics, we have carefully benchmarked it for quantities, such as the band structure, electric-field-driven half-metallicity, and linear optical absorption spectra, against the published *ab initio* works on GNRs, and the results are in very good agreement with each other.

The remainder of this paper is organized as follows. In the next section, we outline the theoretical aspects of our work. In Sec. III, we present and discuss our results. Finally, in Sec. IV, we present our conclusions and discuss the directions for future work.

II. THEORETICAL DETAILS

The PPP-model Hamiltonian,²⁴ with one π electron per carbon atom (half-filled case), is given by

$$H = - \sum_{i,j,\sigma} t_{ij} (c_{i\sigma}^\dagger c_{j\sigma} + c_{j\sigma}^\dagger c_{i\sigma}) + U \sum_i n_{i\uparrow} n_{i\downarrow} + \sum_{i<j} V_{ij} (n_i - 1)(n_j - 1), \quad (1)$$

where $c_{i\sigma}^\dagger$ creates an electron of spin σ on the p_z orbital of carbon atom i , $n_{i\sigma} = c_{i\sigma}^\dagger c_{i\sigma}$ is the number of electrons with spin σ , and $n_i = \sum_\sigma n_{i\sigma}$ is the total number of electrons on atom i . The parameters U and V_{ij} are the on-site and long-range Coulomb interactions, respectively, while t_{ij} is the one-electron-hopping matrix element which, if needed, can be restricted to nearest neighbors (NNs). On setting $V_{ij} = 0$, the Hamiltonian reduces to the Hubbard model. The parametrization of the Coulomb interactions is Ohno-like,²⁶ such that

$$V_{i,j} = U/\kappa_{i,j} (1 + 0.6117 R_{i,j}^2)^{1/2}, \quad (2)$$

where $\kappa_{i,j}$ depicts the dielectric constant of the system which can simulate the effects of screening, and $R_{i,j}$ is the distance in angstroms between the i th and the j th carbon atoms. The Hartree-Fock (HF) theory for periodic one-dimensional systems, within the linear combination of atomic orbitals (LCAO) approach, is fairly standard, and we have implemented both its restricted (RHF) and unrestricted (UHF) variants. The lattice sums are performed in real space by including a large number of unit cells, and integration along the Brillouin Zone (BZ) was performed using the Gauss-Legendre quadrature approach.²⁷ The convergence with respect to the numbers of unit cells included in the lattice sums, as well as k points used for BZ integration, was carefully checked.

Because our calculations, are applications of the PPP model to GNRs in the *bulk* limit, it is important to obtain a suitable set of Coulomb parameters for these systems. In our previous calculations on conjugated molecules and polymers,²⁵ we used two sets of Coulomb parameters, namely (a) ‘‘standard parameters’’ with $U = 11.13$ eV and $\kappa_{i,j} = 1.0$, and (b) ‘‘screened parameters’’ with $U = 8.0$ eV, $\kappa_{i,j} = 2.0$ ($i \neq j$), and $\kappa_{i,i} = 1$, proposed initially by Chandross and Mazumdar to study phenyl-based conjugated polymers.²⁸ In the absence of extensive experimental data, we adopted the criterion of good agreement between the *ab initio* GW band gaps of armchair GNRs (AGNRs)¹³ and our PPP band gaps to choose the Coulomb parameters. The tuning of the parameters was done for AGNR-12 (AGNR- N_A , denoting an AGNR with N_A dimer lines across the width), and with a modified set of screened parameters [$U = 6.0$ eV, $\kappa_{i,j} = 2.0$ ($i \neq j$), and $\kappa_{i,i} = 1$] and an NN-hopping matrix element $t_1 = -2.7$ eV. As a result, good agreement was obtained for AGNR-12 between the PPP band gap (1.75 eV) and the corresponding GW value of Yang *et al.*¹³ Therefore, we have decided to use these modified Coulomb parameters throughout these calculations, with the aim that they will incorporate the GW-level electron-correlation results implicitly in our results.

III. RESULTS AND DISCUSSION

The schematic structures of AGNRs and ZGNRs studied in this work are presented in Fig. 1. Next, we present the results of our PPP-model-based calculations on various quantities for AGNRs and ZGNRs.

A. Band structure

In Fig. 2(a) we present the band structures of AGNR-11 obtained using the Hubbard model with $U = 2.0$ and using the PPP model. At the tight-binding level, all the AGNRs with $N_A = 3p + 2$ (where p is a positive integer) are predicted to be gapless. However, *ab initio* DFT calculations predict all types of AGNRs to be gapped, including those with $N_A = 3p + 2$.^{11,12} Our RHF calculations are in agreement with the DFT results, and also predict all families of AGNRs, including $N_A = 3p + 2$, to be gapped, as is obvious from our PPP results for AGNR-11 presented in Fig. 2(a). The noteworthy point is that the Hubbard model, with the currently accepted values of U , predicts a negligible gap for $N_A = 11$ (cf. Fig. 2(a)), a result in complete disagreement with the DFT and our PPP results. Thus, from this case it is obvious that for AGNRs, long-range Coulomb interactions as included in the PPP model play a very important role of opening up the gap for the $N_A = 3p + 2$ case. Our PPP value of the band gap (1.06 eV) of this AGNR is again in close agreement with the *ab initio* GW result reported by Yang *et al.*¹³

The case of the ground state of ZGNRs is an interesting one with several authors reporting the existence of a magnetic ground state with oppositely oriented spins localized on the opposite zigzag edges of the ribbons,^{6,8} a result verified also in several first-principles DFT calculations.^{11,15} We investigated this in our PPP-model calculations by using the RHF method for the nonmagnetic state and the UHF method for the magnetic one, and the results are summarized in Table I. We find that for a ZGNR of width N_Z ($N_Z \equiv$ number of zigzag lines across the width), abbreviated ZGNR- N_Z , the total energy per cell of the magnetic state (E_m) is lower

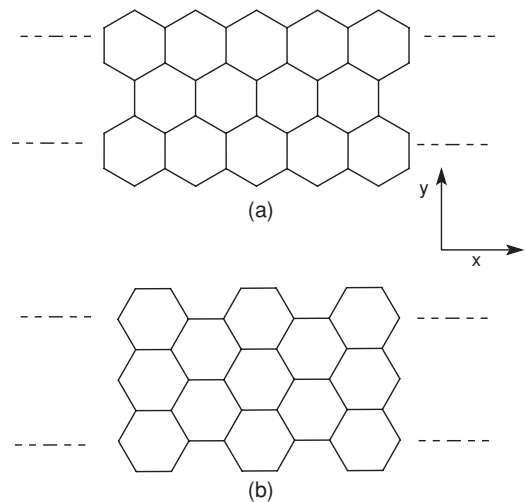


FIG. 1. The structures of (a) a zigzag GNR (ZGNR) and (b) an armchair GNR (AGNR). The ribbons are assumed to lie in the xy plane, with the periodicity in the x direction.

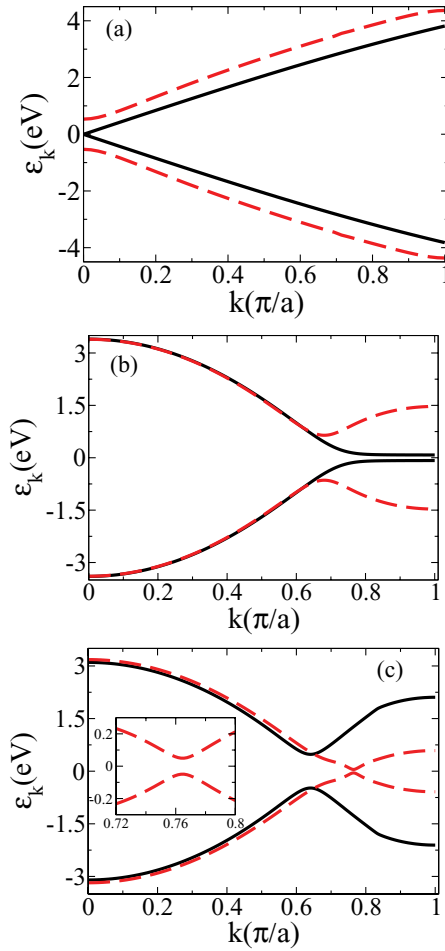


FIG. 2. (Color online) Band structure near the Fermi energy ($E_F = 0$) of (a) AGNR-11 obtained using the Hubbard model (black solid line) with $U = 2.0$ and using the PPP-RHF approach (red dashed line), (b) ZGNR-12 obtained using the PPP-RHF approach for the nonmagnetic state (black solid line) and using the PPP-UHF approach for the magnetic state (red dashed line) in which the bands of up and down spins are degenerate, and (c) ZGNR-16, obtained using the PPP-UHF model, in the presence of a lateral electric field of 0.1 V/\AA so that the up-down degeneracy is lifted (dashed red and solid black bands represent up and down spins, respectively) with $E_g^{m(\text{up})} = 0.11 \text{ eV}$ (magnified in the inset), and $E_g^{m(\text{down})} = 0.97 \text{ eV}$.

compared to that of the nonmagnetic (E_{nm}) one, and the energy difference per atom between the nonmagnetic and the magnetic states [$\Delta E = (E_m - E_{\text{nm}})/N_{\text{at}}$, $N_{\text{at}} \equiv$ number of atoms in the unit cell] decreases with the increasing ribbon width, consistent with the nonmagnetic ground state of graphene. The band gap for the magnetic state (E_g^m) is much larger than that of the nonmagnetic one (E_g^{nm}). The nonzero gaps obtained for the nonmagnetic states of ZGNRs are an artifact of the RHF approach. The band structures of the magnetic and nonmagnetic states of ZGNR-12 computed using the PPP model are presented in Fig. 2(b), and it is obvious that, for the magnetic case, our results are qualitatively very similar to the reported *ab initio* band structures.^{11,15} Quantitatively speaking, for ZGNR-8, we obtain $E_g^m = 1.70 \text{ eV}$, which is higher than the reported GW value of 1.10 eV .¹⁵ Our band gap for AGNR-11

TABLE I. Variation of total energy per cell and the band gaps of ZGNR with the width of the ribbon, computed using the PPP model.

N_z	Total energy (eV)			Band gap (eV)	
	E_{nm}	E_m	ΔE	E_g^{nm}	E_g^m
4	-23.059	-23.261	-0.025	0.524	2.414
6	-35.559	-35.825	-0.022	0.336	2.005
8	-48.103	-48.403	-0.019	0.246	1.694
12	-73.237	-73.570	-0.014	0.161	1.287
16	-98.417	-98.743	-0.010	0.046	1.037

was in excellent agreement with the GW value, but that is not the case with ZGNRs. We believe that it could possibly be because (a) our Coulomb parametrization was based upon *ab initio* GW results¹³ on an AGNR, and (b) electron-correlation effects are stronger in ZGNRs as compared to AGNRs, and the HF approach adopted here ignores those effects.

In a pioneering work, Son *et al.*,¹⁰ based upon *ab initio* DFT calculations, predicted that in the presence of a lateral electric field, ZGNRs exhibit half-metallic behavior leading to their possible use in spintronics. They demonstrated that for the field strength 0.1 V/\AA , the gap for one of the spins of ZGNR-16 will close, leading to metallic behavior for that spin orientation. In Fig. 2(c) we present the band structure of the same ZGNR exposed to the identical field strength, calculated using the PPP model, and the tendency toward half-metallicity is obvious. While the band gap in the absence of the field was 1.037 eV , in the presence of the field, the up-spin band gap is reduced to 0.11 eV , while the down-spin gap decreases to 0.97 eV . Therefore, considering the fact that our PPP-model-based approach does not incorporate electron-correlation effects, its quantitative predictions are in very good agreement with the *ab initio* ones,¹⁰ and thus it is able to capture the essential physics of the electric-field-driven half-metallicity in ZGNRs.

B. Optical absorption

Next we present the linear optical absorption spectra of GNRs, computed within the PPP model. The optical absorption spectrum for the x -polarized (y -polarized) photons is computed in the form of the corresponding components of the imaginary part of the dielectric constant tensor, i.e., $\epsilon_{xx}^{(2)}$ [$\epsilon_{yy}^{(2)}$], using the standard formula

$$\epsilon_{ii}^{(2)}(\omega) = C \sum_{v,c} \int_{-\pi/a}^{\pi/a} \frac{|\langle c(\mathbf{k}) | p_i | v(\mathbf{k}) \rangle|^2}{\{[E_{cv}(\mathbf{k}) - \hbar\omega]^2 + \gamma^2\} E_{cv}^2(\mathbf{k})} d\mathbf{k}, \quad (3)$$

where a is the lattice constant, p_i denotes the momentum operator in the i th Cartesian direction, ω represents the angular frequency of the incident radiation, $E_{cv}(\mathbf{k}) = \epsilon_c(\mathbf{k}) - \epsilon_v(\mathbf{k})$, with $\epsilon_c(\mathbf{k})$ [$\epsilon_v(\mathbf{k})$] being the conduction band (valence band) eigenvalues of the Fock matrix, γ is the linewidth, while C includes the rest of the constants. We have set $C = 1$ in all the cases to obtain the absorption spectra in arbitrary units. The components of the momentum matrix elements $\langle c(\mathbf{k}) | \mathbf{p} | v(\mathbf{k}) \rangle$

needed to compute $\epsilon_{ii}^{(2)}(\omega)$, for a general three-dimensional system, can be calculated using the formula²⁹

$$\langle c(\mathbf{k})|\mathbf{p}|v(\mathbf{k})\rangle = \frac{m_0}{\hbar} \langle c(\mathbf{k})|\nabla_{\mathbf{k}}H(\mathbf{k})|v(\mathbf{k})\rangle + \frac{im_0[\epsilon_c(\mathbf{k}) - \epsilon_v(\mathbf{k})]}{\hbar} \langle c(\mathbf{k})|\mathbf{d}|v(\mathbf{k})\rangle, \quad (4)$$

where m_0 is the free-electron mass, $\nabla_{\mathbf{k}}H(\mathbf{k})$ represents the gradient of the Hamiltonian (Fock matrix, in the present case) in \mathbf{k} space, and $\langle c(\mathbf{k})|\mathbf{d}|v(\mathbf{k})\rangle$ denotes the matrix elements of the position operator \mathbf{d} defined with respect to the reference unit cell and accounts for the so-called intra-atomic contribution.²⁹ Note that Eq. can also be used to compute the matrix element $\langle c(\mathbf{k})|p_y|v(\mathbf{k})\rangle$ needed to compute the absorption spectrum for the y -polarized light for GNRs (which are periodic only in the x direction) by setting the first term on its right-hand side to zero, because for a one-dimensional system periodic along the x direction, the Hamiltonian has no k_y dependence. $\langle c(\mathbf{k})|\nabla_{\mathbf{k}}H(\mathbf{k})|v(\mathbf{k})\rangle$ for the case of GNRs is obtained easily by calculating the numerical derivative of the Fock matrix at various k points of the one-dimensional BZ. For the \mathbf{d} operator, the usual diagonal representation was employed. With regards to the absorption spectra of the GNRs for the y -polarized photons [$\epsilon_{yy}^{(2)}(\omega)$], because such transverse excitations do not couple to the photons polarized along the x direction, they have also been called “dark excitons” in the literature.^{13,15}

The optical absorption in AGNRs has been studied extensively by *ab initio* approaches in recent works.^{12,13,16} In Fig. 3(a) we present the optical absorption spectrum of the AGNR-11. If Σ^{mn} denotes a peak in the spectrum due to a transition from the m th valence band (counted from the

top) to the n th conduction band (counted from the bottom), the peak of $\epsilon_{xx}^{(2)}(\omega)$ at 1.1 eV is Σ^{11} , at 3.1 eV is Σ^{22} , at 3.8 eV is Σ^{33} , and at 5.8 eV is Σ^{44} . The peaks of $\epsilon_{yy}^{(2)}(\omega)$ at 2.1 and 5.6 eV correspond to Σ^{12} and Σ^{21} , respectively. The remarkable feature of the presented spectrum is that, owing to the symmetry of the AGNRs, the peaks corresponding to x - and y -polarized photons are well separated in energy, and their relative intensities can be measured by performing experiments on oriented samples. On comparing our PPP spectrum [$\epsilon_{xx}^{(2)}(\omega)$] with the *ab initio* GW spectrum of Yang *et al.*,¹³ we note that the locations of the first peaks close to 1.1 eV are in excellent agreement with each other. However, our calculations predict several higher energy peaks with significant intensities located around 3.0 eV that are absent in the GW work. Furthermore, we also predict the intensities of the y -polarized peaks, which were absent in the work of Yang *et al.*¹³

In Fig. 3(b) we present our calculated optical absorption spectrum [$\epsilon_{xx}^{(2)}(\omega)$ and $\epsilon_{yy}^{(2)}(\omega)$] for the ZGNR-8. The peaks in $\epsilon_{xx}^{(2)}(\omega)$ are located at 1.7 eV (Σ^{11}), 2.9 eV ($\Sigma^{12} + \Sigma^{21}$), and 4.0 eV (Σ^{22}), while the prominent peaks of $\epsilon_{yy}^{(2)}(\omega)$ are at 1.7 eV (Σ^{11}) and 2.9 eV ($\Sigma^{12} + \Sigma^{21}$). The noteworthy point is that most of the prominent peaks have mixed polarization characteristics, unlike the case of AGNRs. This is because of the fact that for magnetic ground states, the reflection about the xz plane is broken, leading to mixed polarizations. This is an important result which can also be tested in oriented samples of ZGNRs. Our PPP optical absorption spectrum of this ZGNR compares qualitatively well to the GW spectrum computed by Yang *et al.*¹⁵, although our peaks are consistently blue-shifted compared to the GW result, due to the corresponding

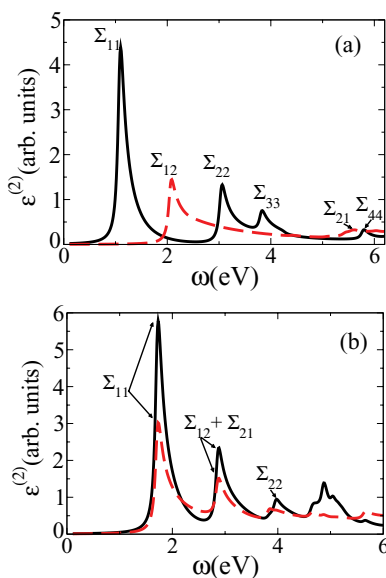


FIG. 3. (Color online) Imaginary parts of the dielectric constant [$\epsilon_{xx}^{(2)}(\omega)$ in black solid and $\epsilon_{yy}^{(2)}(\omega)$ in red dashed lines] computed using the PPP model and modified screened parameters, for (a) AGNR-11 and (b) ZGNR-8, with a magnetic ground state. Labels of the peaks denote the bands involved in the transition (see text for an explanation), and a linewidth of 0.05 eV was assumed throughout.

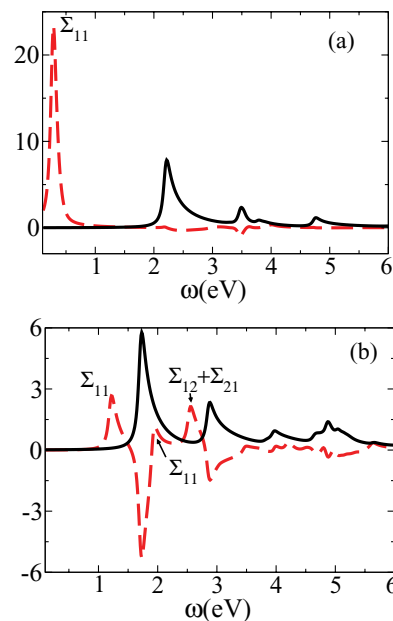


FIG. 4. (Color online) Linear absorption spectrum (black solid) and electroabsorption spectrum (red dashed) of ZGNR-8 for photons polarized along the x axis for (a) the nonmagnetic ground state and (b) the magnetic ground state. A linewidth of 0.05 eV was assumed throughout, and the bands involved in the EA peaks are indicated.

disagreement in the band structure. Moreover, Yang *et al.*¹⁵ did not compute the peak intensities for the y -polarized photons.

C. Electroabsorption

In Fig. 4 we present the EA spectrum of ZGNR-8 computed as the difference of the linear absorption spectra with and without an external static E field of strength 0.1 V/\AA along the y axis. In Fig. 4(a) we present the EA spectrum for the nonmagnetic ground state of ZGNR-8, computed using the PPP-RHF approach. Without the external E field, the Σ_{11} transition is disallowed for the nonmagnetic state of such a ZGNR for the x -polarized light due to symmetry selection rules.¹⁴ However, in the presence of the field, due to the broken symmetry, this transition becomes strongly allowed, leading to a very strong peak in the EA spectrum. Figure 4(b) portrays the EA spectrum of the same ZGNR for the magnetic ground state, and here the physics of half-metallicity manifests itself in that one observes two energetically split peaks corresponding to two different Σ_{11} transitions among up- and down-spin electrons. Thus, our calculations predict that the EA signal is different for the ZGNRs depending on whether they have a magnetic or a nonmagnetic ground state, a result which can be used to determine the nature of the ground state of ZGNRs using EA spectroscopy.

IV. SUMMARY AND OUTLOOK

In summary, we have used a PPP-model-based π -electron approach, incorporating long-range Coulomb interactions, to study the electronic structure and optical properties of

GNRs in the bulk limit. In particular, we computed the optical absorption spectra of GNRs for transversely polarized photons, in addition to the longitudinal ones, thereby allowing us to investigate the anisotropic optical response of these materials. Our predictions that for AGNRs longitudinal and transverse polarized components will be well separated energetically, while ZGNRs will exhibit absorption with mixed polarization, can be tested in experiments on oriented samples. Furthermore, we also presented calculations of the EA spectra of ZGNRs, and our results suggest a possibility of an optical determination of whether or not they possess a ground state with edge magnetism.

It will also be of interest to perform similar studies on bilayer and other multilayer GNRs, to investigate how various properties of the ribbons evolve as the number of layers are increased. Of particular interest is the case of multilayer ZGNRs to probe the nature of edge magnetism in those systems. Furthermore, it will also be of interest to include excitonic effects in the optical absorption spectrum of ZGNRs so as to perform a complete comparison with the future experimental work on these systems. For that purpose, it is important to go beyond the HF approach and include electron-correlation effects. Work along all these directions is in progress in our group, and the results will be communicated in future publications.

ACKNOWLEDGMENTS

We acknowledge the Department of Science and Technology (DST), Government of India, for providing financial support for this work under Grant No. SR/S2/CMP-13/2006. K.G. acknowledges S. V. G. Menon of the Bhabha Atomic Research Centre (BARC) for his continued support of this work.

*Permanent Address: Theoretical Physics Division, Bhabha Atomic Research Centre, Mumbai 400085, India; naiduk@barc.gov.in, shukla@iitb.ac.in

¹K. S. Novoselov, A. K. Geim, S. V. Morozov, D. Jiang, Y. Zhang, S. V. Dubonos, I. V. Grigorieva, and A. A. Firsov, *Science* **306**, 666 (2004).

²Y. Zhang, Y.-W. Tan, H. L. Stormer, and P. Kim, *Nature (London)* **438**, 201 (2005).

³K. S. Novoselov, A. K. Geim, S. V. Morozov, D. Jiang, M. I. Katsnelson, I. V. Grigorieva, S. V. Dubonos, and A. A. Firsov, *Nature (London)* **438**, 197 (2005).

⁴K. S. Novoselov, Z. Jiang, Y. Zhang, S. V. Morozov, H. L. Stormer, U. Zeitler, J. C. Maan, G. S. Boebinger, P. Kim, and A. K. Geim, *Science* **315**, 1379 (2007).

⁵M. Y. Han, B. Özyilmaz, Y. Zhang, and P. Kim, *Phys. Rev. Lett.* **98**, 206805 (2007); Z. Chen, Y.-M. Lin, M. J. Rooks, and P. Avouris, *Physica E* **40**, 228 (2007); K. A. Ritter and J. W. Lyding, *Nature Mater.* **8**, 235 (2009); J. Cai *et al.*, *Nature (London)* **466**, 470 (2010).

⁶M. Fujita, K. Wakabayashi, K. Nakada, and K. Kusakabe, *J. Phys. Soc. Jpn.* **65**, 1920 (1996).

⁷K. Nakada, M. Fujita, G. Dresselhaus, and M. S. Dresselhaus, *Phys. Rev B* **54**, 17954 (1996).

⁸S. Okada and A. Oshiyama, *Phys. Rev. Lett.* **87**, 146803 (2001).

⁹M. Ezawa, *Phys. Rev. B* **73**, 045432 (2006).

¹⁰Y. W. Son, M. L. Cohen, and S. G. Louie, *Nature (London)* **444**, 347 (2006).

¹¹Y. W. Son, M. L. Cohen, and S. G. Louie, *Phys. Rev. Lett.* **97**, 216803 (2006).

¹²V. Barone, O. Hod, and G. E. Scuseria, *Nano Lett.* **6**, 2748 (2006).

¹³L. Yang, M. L. Cohen, and S. G. Louie, *Nano Lett.* **7**, 3112 (2007).

¹⁴H. Hsu and L. E. Reichl, *Phys. Rev. B* **76**, 045418 (2007).

¹⁵L. Yang, M. L. Cohen, and S. G. Louie, *Phys. Rev. Lett.* **101**, 186401 (2008).

¹⁶D. Prezzi, D. Varsano, A. Ruini, A. Marini, and E. Molinari, *Phys. Rev. B* **77**, 041404 (2008).

¹⁷See e.g., M. Liess, S. Jeglinski, Z. V. Vardeny, M. Ozaki, K. Yoshino, Y. Ding, and T. Barton, *Phys. Rev. B* **56**, 15712 (1997).

¹⁸A. H. Castro Neto, F. Guinea, N. M. R. Peres, K. S. Novoselov, and A. K. Geim, *Rev. Mod. Phys.* **81**, 109 (2009).

¹⁹J. Fernández-Rossier and J. J. Palacios, *Phys. Rev. Lett.* **99**, 177204 (2007).

²⁰O. V. Yazyev, *Phys. Rev. Lett.* **101**, 037203 (2008).

²¹J. Jung and A. H. MacDonald, *Phys. Rev. B* **79**, 235433 (2009).

²²A. Yamashiro, Y. Shimo, K. Harigaya, and K. Wakabayashi, *Phys. Rev. B* **68**, 193410 (2003).

²³L. Salem, *The Molecular Orbital Theory of Conjugated Systems* (Benjamin, New York, 1966).

- ²⁴J. A. Pople, *Trans. Faraday Soc.* **49**, 1375 (1953); R. Pariser and R. G. Parr, *J. Chem. Phys.* **21**, 466 (1953).
- ²⁵See e.g., P. Sony and A. Shukla, *Phys. Rev. B* **75**, 155208 (2007); *J. Chem. Phys.* **131**, 014302 (2009); *Comput. Phys. Comm.* **181**, 821 (2010), and references therein.
- ²⁶K. Ohno, *Theor. Chim. Acta* **2**, 219 (1964).
- ²⁷J. M. André, D. P. Vercauteren, V. P. Bodart, and J. G. Fripiat, *J. Comput. Chem.* **5**, 535 (1984).
- ²⁸M. Chandross, S. Mazumdar, M. Liess, P. A. Lane, and Z. V. Vardeny, M. Hamaguchi, and K. Yoshino, *Phys. Rev. B* **55**, 1486 (1997).
- ²⁹T. G. Pedersen, K. Pedersen, and T. B. Kristensen, *Phys. Rev. B* **63**, 201101(R) (2001).